

See discussions, stats, and author profiles for this publication at: <https://www.researchgate.net/publication/303430672>

A framework of synthetic aperture radar imaging based on iterative reweighted compressed sensing

Article · June 2015

DOI: 10.5013/IJSSST.a.16.03.15

CITATION

1

READS

9

3 authors:



Rahmat Arief

Indonesian National Institute of Aeronautics and Space

12 PUBLICATIONS 8 CITATIONS

[SEE PROFILE](#)



Dodi Sudiana

University of Indonesia

54 PUBLICATIONS 94 CITATIONS

[SEE PROFILE](#)



Kalamullah Ramli

University of Indonesia

119 PUBLICATIONS 189 CITATIONS

[SEE PROFILE](#)

Some of the authors of this publication are also working on these related projects:



University Priority Research Grant [View project](#)



International Publication Research Grant [View project](#)

A Framework of Synthetic Aperture Radar Imaging based on Iterative Reweighted Compressed Sensing

Rahmat Arief^{1,2}, Dodi Sudiana¹, Kalamullah Ramli¹

¹ *Department of Electrical Engineering*
Universitas Indonesia
Depok 16424, Indonesia
e-mail: rahmat.arief@ui.ac.id, rahmat.arief@lapan.go.id

² *Remote Sensing Division*
Indonesian National Institute of Aeronautics and Space
(LAPAN), Jakarta 13710, Indonesia

Abstract — Synthetic aperture radar system has an ability to generate high resolution image data. It requires high rate data acquisition, huge data storage, high power consumption and high onboard resources complexity. Compressive sensing offers solution to overcome those problems. A new framework of SAR image formation is proposed for sparse targets based on compressed sensing. It allows a compressed sampling with a very few of SAR echo samples required under Nyquist / Shannon theorem of both slow time and fast time radar signals and uses Iterative Reweighted Least Square Lp-minimization algorithm for image reconstruction in the noisy environment. Analysis was conducted by comparing the imaging results of SAR point target with different number of under sampling measurement and signal noise ratio level. The results showed that this approach is able to produce reconstructed sparse image with reduced side lobe and noise as compared to iterative reweighted L1 and respectively L2.

Keywords - synthetic aperture radar; compressive sensing; iterative reweighted least square; lp-minimization

I. INTRODUCTION

Synthetic Aperture Radar (SAR) sensor can be operated to generate high resolution image data of target from a moving platform at night and on all-weather condition [1], [2]. Most of SAR images have characteristic of sparse or compressible in proper basis. It is possible to solve the problem with compressive sensing (CS) method, that the SAR image of sparse targets can be recovered by solving the convex optimization problem with a very few of SAR echo samples required under Nyquist/Shannon theorem [3–5].

Several studies have addressed on a linear modeling of SAR signal i.e. Herman [6] proposed a linear model of the SAR signal with Alltop-sequence models and Wei [7] derived SAR echo signal by separation of targets from SAR raw data. Another approach of linear model of SAR raw data is derived from Maxwell equations [8–11]. Other studies of CS applications for SAR data have been proposed. [6], [7], [12–14] state that the schemes using CS in SAR can eliminate the match filter [12], reduce bandwidth ADC [12], reduce noise and minimize the effects of side lobes in the radar [7].

L1-minimization [12], [14] used widespread in the recovery of sparse SAR image and offers a solution of convex optimization problem with exact recovery of sparse signal. Several methods have been introduced for finding optimally sparse representation of non-convex optimization problem, i.e. iterative reweighting schemes, which produce more accurate estimations. Variants of reconstruction algorithm to solve certain optimization problems are iterative reweighted L1 (IRL1) [15] and iterative reweighted L2 (IRL2) [16]. Several works showed that the proposed CS SAR processing methods have advantages compared to the conventional SAR imaging method.

In this paper, we introduce a new framework of SAR image formation for sparse target based on compressive sensing method in noisy environment. The framework consists a linear modeling of SAR signal, a scheme of sampling method of SAR signals on both slow time (azimuth) and fast time (range) sampling and SAR image reconstruction using iterative reweighted least square–Lp (IRLS–Lp) minimization.

II. COMPRESSIVE SENSING

If a signal can be expressed by a complete system of basis vectors ψ_1, \dots, ψ_2 and assumed to be linear, then the signal can be written as follow [3–5]

$$s(t) = \sum x_i \psi_i(t) \quad \text{or} \quad s = \Psi x \quad (1)$$

where Ψ is the matrix composed of the $N \times 1$ column vectors ψ_i , where index of target $i = 1 \dots J$, The measured signal s is $N \times 1$ vector, which might be sparse in a certain representation with basis Ψ and the coefficient vector x is an $J \times 1$ unknown sparse vector with small numbers of K non-zero components.

The Nyquist-Shannon sampling theorem assumes that the signal s is band limited, and can be recovered without loss by sampling at sampling rate which is greater than two times their bandwidth signal ($2 \cdot f_0$) [17]. Nyquist-Shannon sampling theorem ignores the sparsity of the elements of the vector x . This led to a large amount of data in imaging systems.

The CS enables the reconstruction of sparse vector x from a smaller set of linear measurements of s than required under Nyquist/Shannon sampling theorem [3]. In this case s is compressible signal. In a compressed sensing framework,

the signal is acquired through compressive sampling, which is formulated as undersampled measurement of \mathbf{s} from Eq. (1) via linear random procedure as follows [3–5]

$$\mathbf{y} = \Phi \mathbf{s} = \Phi \Psi \mathbf{x} + \mathbf{n} \quad (2)$$

where $\mathbf{y} \in \mathbb{R}^M$ is the compressed measurement vector, $\Phi \in \mathbb{R}^{M \times N}$ is referred to as the random measurement matrix, which forms an incomplete basis ($M < N$) and \mathbf{n} is measurement noise. A good measurement matrix can provide the information in \mathbf{x} and the signal \mathbf{x} can be recovered exactly from \mathbf{y} by solving an regularized L1-minimization problem [18].

$$\hat{\mathbf{x}} = \min_{\mathbf{x}} \frac{1}{2} \|\mathbf{y} - \Phi \Psi \mathbf{x}\|_2^2 + \lambda \|\mathbf{x}\|_1, \lambda > 0 \quad (3)$$

The $\|\cdot\|_1$ denotes L1-norm, λ is scalar regulation parameter and the rows of Φ chosen in form of vectors in M dimension and the sensing matrix $\mathbf{A} = \Phi \Psi$ has the Restricted Isometry Property (RIP) [3], [4]. In order to recover a K -sparse vector \mathbf{x} , the number of measurements M ($K < M \ll N$) must be selected at least greater than K but can be significantly smaller than the length of signal (N) with $M \geq C_1 K \log(N/K)$.

III. PROPOSED FRAMEWORK OF SAR IMAGING BASED ON CS

A. SAR Signal Model

High-resolution images can be produced in Stripmap SAR operation mode with a relatively small antenna by moving the antenna at a constant velocity with respect to the target. SAR imaging can be formulated as a linear inverse problem, which is retrieved from noisy measurements of backscattered radar signals of object targets.

SAR systems use a pulsed Linear Frequency Modulated (LFM) waveform, referred to as a chirp signal. The LFM waveform has good pulse compression properties. It is assumed that a single pulse is given as follow

$$s_T(t) = A_0 \text{rect}\left(\frac{t}{T_p}\right) \cdot e^{j\pi f_c t + j\pi K t^2} \quad (4)$$

where A_0 amplitude, t time, T_p pulse duration, f_c carrier frequency, K chirp rate and $\text{rect}(\cdot)$ is the rectangular window function.

Radar transmits many of these pulses that are separated in pulse repetition interval. During the receiving duration, the antenna waits to receive reflected radar signals from the targets contained in a one-dimensional range slice echo. The received signal is the original transmitted signal, which is time delayed, attenuated, phase shifted amplitude modified due to azimuth beam pattern affects and is contained additive noise. The raw SAR received radar signal is assumed as a baseband signal after quadrature demodulation which removes the high frequency carrier wave. Quadrature demodulation causes the signal to be imaginary and have a

phase and a magnitude. As observed in [8], the received baseband signal is formulated as:

$$s_{\text{RB}}(t_n, \eta_j) = \sum_{j=1}^J x_j |\text{rect}(t_n - \tau_{\eta_j})|^2 e^{-j2\pi f_c \tau_{\eta_j} + j\pi K (t_n - \tau_{\eta_j})^2} + \mathbf{n} \quad (5)$$

where x_j is scattering coefficient, $j = 1 \dots J$ is index of scattering response, J is the total number of targets, $\tau_j = \frac{2R_j}{c}$ is time delay of echo, t_n fast time and η_j slow time where index $j = 1, \dots, N_s$, $n = 1, \dots, N_T$. N_s and N_T are the total number of samples required under Nyquist theorem of slow time and fast time signal respectively. A measurement noise \mathbf{n} is regarded as additive white Gaussian noise. The distance R_j between the radar sensor at position (x_r, y_r) and each scattering response at all spatial location (x_j, y_j) can be computed as

$$R_j = \sqrt{(\eta_j^2 - y_r^2) + (h^2 + (x_r + x_j)^2)} \quad (6)$$

where h is height of the radar sensor and x_r is the range of center of target.

B. Linear Measurement Model

The requirement that must be satisfied in CS method is that the signal to be sparse or compressible signals in a particular domain. The received SAR signal may not have a sparse property in time domain, but the scene could be sparse in different domain. The simplest form of sparsity in the SAR imaging would be a scene containing of a few numbers of dominant scatterers e.g. ships at ocean.

The sparse representation from backscattered signal as derived from (5) as explained in the following. As assumed, $x_j \in \mathbb{C}^{N_s}$ are scattering coefficients which indicate the magnitude of complex signal in 1D with a small number of K dominant scatterers in a vector length J . A linear measurement model of SAR signal is formulated by separating the components of matrix of SAR signal model Ψ dan scattering coefficient x_j from the formula

$$s_{\text{RB}}(t_n, \eta_j) = \sum_{j=1}^J x_j \omega_j e^{-j\varphi_j(t_n, \eta_j)} + \mathbf{n}_B \quad (7)$$

where

$$\omega_j = |\text{rect}(t_n - \frac{2R_{\eta_j}}{c})|^2$$

$$\varphi_j(t_n, \eta_j) = 4\pi f_c \frac{R_{\eta_j}}{c} - \pi K (t_n - \frac{2R_{\eta_j}}{c})^2$$

The vector \mathbf{s}_{RB} can be simplified in the form of a linear model equation as below

$$\mathbf{s}_{\text{RB}} = \Psi \mathbf{x} + \mathbf{n}_B \quad (8)$$

where

$$\Psi = [\psi_1, \psi_2, \dots, \psi_J] \text{ and}$$

$$\varphi_j(t_n, \eta_l) = [\omega_j e^{-j\varphi_1(z, \Delta)}, \dots, \omega_j e^{-j\varphi_1(z, N_r)}, \omega_j e^{-j\varphi_1(z, \Delta)}, \dots, \omega_j e^{-j\varphi_1(z, N_r)}]^T$$

Ψ is a mathematical model of SAR signal acquisition in the form of a matrix with dimension of $N_s \times J$ as orthonormal basis, where $N_s = N_a \times N_r$ and J is the total number of targets.

C. *Undersampling on SAR Data*

In order to show the effectiveness of recovery performance from CS algorithms on a sparse SAR scene x , a few of random measurement of received SAR signal S_{RB} is formed as follows,

$$y = \Phi S_{RB} = \Phi \Psi x + n \tag{9}$$

where y fewer random measurement, Φ measurement matrix with size $M \times N_s$ which is constructed randomly. The number of measurements M must be selected at least greater than K but can be significantly smaller than the scene dimension N_s ($K \ll M \ll N_s$).

The SAR image is formed from each backscattered signal in the fast time and in the slow time directions. A few measurement of y in SAR raw echoes can be generated in 2 steps: (1) under sampling of SAR raw echoes in fast time is generated by receiving fewer backscattered pulses randomly than conventional system; (2) under sampling in slow time is generated by receiving backscattered pulses from randomly fewer transmitted radar pulses.

Figure 1 describes the under sampling method of SAR raw echoes from ideal point targets (a) full sampling of point target raw echo; (b) under sampling in slow time; (c) under sampling in fast time; (d) combination under sampling in fast time and slow time. The proposed framework used the (d) under sampling method, which will reduce the most the number of samples.

D. *Algorithm of Iterative Reweighted Least Square – Lp-Minimization*

In most cases, to find the approximation of sparse SAR scene from a few of random samples number in noisy SAR raw data can be done by solving (3) efficiently. Several recent approximation algorithms rely on iterative reweighted algorithm such as IRL1-[15] and IRL2-[16].

Sparse SAR signal can be recovered by solving the inverse problem using the general LS-Lp minimization model for unconstrained problem:

$$\min_x \frac{1}{2} \|y - \Phi \Psi x\|_2^2 + \lambda \|x\|_{p, \epsilon}^p \tag{10}$$

We consider that the Lp-norm as our objective optimization function as

$$\|x\|_{p, \epsilon}^p = \sum_1^J (x_j^2 + \epsilon)^{p/2} \tag{11}$$

where $\epsilon \geq 0$, is a regulation factor that is selected to improve the ability of (10) to recover the sparsed scene as iteration increased. We substitute

(11) into (10) to represent the sparse signal problem, which minimizes the Lp-norm function:

$$\min_x \frac{1}{2} \|y - \Phi \Psi x\|_2^2 + \lambda \sum_1^J (x_j^2 + \epsilon)^{p/2} \tag{12}$$

The minimization problem could be solved since

$$\min_x \frac{1}{2} \|y - \Phi \Psi x\|_2^2 + \lambda \sum_1^J (x_j^2 + \epsilon)^{p/2} \tag{12}$$

is continuous with respect to x . The minimum solution over x is obtained by equalizing the first order derivative of (12) to zero, which yields the solution of $x^{(k+1)}$ at $(k+1)$ -th iteration as follow.

$$x^{(k+1)} = \text{inv}[\Psi^T \Phi^T \Phi \Psi + p \cdot \tilde{W}^{(k)}] \Psi^T \Phi^T y \tag{13}$$

where $\tilde{W}^{(k)}$ is a diagonal weighting matrix of $(k+1)$ -th iteration with diagonal element $1/w_j^{(k)}$ and $w_j^{(k)} = \lambda / (x_j^{(k)2} + \epsilon^{(k)})^{1-p/2}$ depends on the previous value of x . A diagonal weighting matrix is expressed as $\tilde{W}^{(k)}$ and defined as

$$\tilde{W}^{(k)} = \text{diag} \left(\frac{\lambda}{(x_j^{(k)2} + \epsilon^{(k)})^{1-p/2}} \right) \tag{14}$$

We consider that the approach is non-convex optimization problem, when $p \in [0, 1]$. In this algorithm, the approximation of the sparse solution scene $x^{(k+1)}$ is computed as the magnitude of complex value by choosing user defined p and updating of $\epsilon^{(k)}$ as the iteration increased. As observed in [15], the factor ϵ is chosen as a constant, but in [16], ϵ is expressed as $\epsilon^{(k)} \geq 0$, that it is reduced to zero as the iteration increased.

For noiseless case, it is assumed that the regulation parameter is fixed $\lambda \rightarrow 0$, while it is larger for noisy condition [16]. As observed in [19], supposed that the measurement is obtained in (9) where the entries of n are $N(0, \sigma^2)$, λ is a function of the variance of noise σ^2 , then λ is expressed as

$$\lambda = \sqrt{8\sigma^2(1 + \alpha) \log(N - K)} \tag{15}$$

where α is small value $\alpha > 0$.

The approximated scene $x^{(k+1)}$ is obtained when the iteration is stopped in a condition that the iteration number reaches maximum or the difference between the current $x^{(k+1)}$ and previous $x^{(k)}$ reached the defined error tolerance value.

The solution of sparse SAR image processing framework based on Iterative Reweighted Least Square – Lp (IRLS-Lp) minimization algorithm is summarized in algorithm 1.

Require	: SAR raw echoes s , matrix of SAR signal acquisition model Ψ , random undersampling operator Φ ,
Ensure	: Reconstructed SAR image $x^{(k+1)}$
Initial	: Noise level, energy min $x^{(0)}$, error tolerance, p and max iteration it_{max}
Step of solution	: define under sampling measurement y define start value of ϵ (epsilon)

```

define decrease_factor
define regulation parameter  $\lambda$ 
while (k=1 to  $k_{max}$  or  $\text{norm}(x^{(k+1)} - x^{(k)}) \leq \epsilon Tol$ )
    define weighting factor  $\Psi^{(k)}$  in (14)
    create new approximated result  $x^{(k+1)}$  using (13)
    define  $\epsilon^{(k+1)} = \epsilon^{(k)} / \text{decrease\_factor}$ 
end
    
```

Algorithm. 1 The proposed sparsed SAR image formation using IRLS-Lp minimization algorithm

IV. RESULT AND ANALYSIS

This section describes a performance demonstration of SAR image processing framework based on IRLS-Lp Minimization algorithm. As a comparison of the recovery performance of the proposed framework, we used SAR image processing method based on L1[20], IRL1[15] and IRL2[16]. We present the results of the proposed framework in experiments with SAR scenes of point target. The input is a selected target from a two-dimensional target profile of reflectivity over the azimuth and range based on the intensity of the pixels in the target image.

In the first experiment, we demonstrate the performance of the proposed framework on sparse SAR signal in different measurement numbers of sampling. The target scene consist points or objects with different scattering response in a 32x32 pixel image. The important parameters of SAR stripmap mode are 10 GHz frequency center with 1.00 m of azimuth and range resolution respectively. First, we generate SAR raw echoes s and the SAR acquisition basis vector Ψ from a target scene. Then the echo signals are added by Gaussian white noise. For full sampling, the radar signals were acquired with sampling rate as required by the Nyquist theorem. We obtained the size of SAR raw echoes $N_s = 96 \times 126$, which means the maximum number of samples in azimuth and range axis $N_a = 96$ and $N_r = 126$ respectively.

The experimental setup uses input data of 9 target points with noise of 10 dB. The parameters used to run the experiment are as follows: (a) the value $p=0.1$; (b) the start value of ϵ selected with the initial value of 1 and changed decreasing factor of 5 at the time if the iteration increases; (c) λ is determined fixed as (15); (d) Experiments performed iteratively and stopped if the difference between the current and previous reconstructed scene is less than the error tolerance ($\epsilon Tol = 1e^{-3}$). If the iteration goes on and error tolerance value is not reached, then the experiment is terminated by the stopping criteria as the maximum number of iterations is reached (maximum iteration = 25). Random measurements were conducted as compressed sampling in the azimuth and range as $M=(60,70,80,90)$ samples of the total number of sampling $N_s = 12096$. It means, if the number of non-zero component $K=9$, compression ratio between number of random measurements M compared to total number of signal N_s is 0.5% - 0.74 % to get the good approximated scene. Figure 2 showed the comparison of approximated scenes using previous and our proposed method.

The SAR image quality is obtained by measuring the reconstruction error using Root Mean Square Error (RMSE) and Pseudo Signal to Noise Ratio (PSNR). Figure 2 illustrated the result of sparse SAR scene of ideal point target response using iterative reweighted CS algorithms. The result of reconstructed scenes shows the reduction of side lobes and noise on the L1, IRL1, IRL2 and IRLS-Lp minimization based reconstruction when the number of measurements increases. The point targets are easily seen visually, that the proposed framework resulted in reduced noise and much sharper image because of reduced side lobes in noisy environments. The comparison between algorithms can be viewed also from RMSE and PSNR value of the recovery results (see figure 3). If the number of measurements increases, the recovery ability of all methods is also increased. The proposed algorithm shows improved performance compared to L1-, IRL1-, IRL2- based reconstruction

We also demonstrated the performance of new framework of SAR image formation using IRLS-Lp minimization algorithm on sparse SAR signal in noisy condition. The same SAR raw data in the previous experiment is added with different level of gaussian noise ranging from the highest noise level (SNR=5dB) to the lowest noise level (SNR=40 dB). The setup parameters used in this experiment are the same as previous with the number of measurement of $M=100$. Figure 4 showed that the noise affects the quality of the approximated scene. High level noise on SAR raw data reduces the quality of reconstructed SAR imagery and our framework performed denoising process better even at high level noise condition compared to other algorithms.

From these results, we analyze the performance of the framework based on a number of parameters: p , λ and ϵ .

A. Selection of p value

Choosing of correct value of p affects the framework to estimate the approximated scenes. Small values of p resulted in small reconstruction error value, which is better than larger one. Figure 5 showed the approximated scene is almost exactly fully recovered by choosing $p \leq 0.3$ with a small RMSE value and high PSNR value in any noisy environments. Lower the noise level resulted in smaller RMSE and higher PSNR of the approximated scenes and vice versa. The selection of p also affects the speed of calculation of the approximated scenes to the convergence criteria and shortens the time or reduces number of iterations.

B. Regulation parameter λ

The regulation parameter λ in (15) depends on variance σ^2 of noise level of the original signal and other parameters such small value of α , signal length n and k -sparse. Higher noise resulted in larger λ . In noiseless case the regulation parameter λ is assumed fixed to zero ($\lambda \rightarrow 0$). If the number of k - non zero components too small compared to the signal length n , then $\lambda = \sqrt{8\sigma^2(1+\alpha)\log(n)}$.

C. Regulation parameter ϵ

Regulation parameter ϵ for weighting factor W is chosen such that a global minimum value in non convex problems can be found promptly by increasing iteration. The value of ϵ is chosen with an initial value and decrease towards zero with increasing iteration by decrease factor $\epsilon^{(k+1)} = \epsilon^{(k)} / \text{decrease_factor}$. If the decrease factor has been declining too slowly, it will lead to bad estimation of the approximation scenes.

Figure 6 showed that good approximated scenes are obtained for decrease factor of ϵ larger than 3.0. We set the initial value of $\epsilon = 1$ and decrease factor of 2.0 to 5.0 to get a good comparison of approximated scene using IRLS-Lp algorithm in different level of noise.

V. CONCLUSION

This paper described the proposed framework of sparse SAR image formation based on iterative reweighting CS algorithm. The framework is able to reconstruct the sparse SAR signal with low sampling rate both in azimuth and range in noisy environments. We found that (1) the performance of CS recovery algorithms depends on the number of measurement and the input SNR (2) The proposed IRLS-Lp minimization method has better performance compared to other methods L1, IRL1 and IRL2. (3) The proposed framework is able to perform better denoising process as well as reducing the side lobes even at high noise condition. (4) One of the advantages of the proposed algorithm compared with IRL1 and IRL2 is the freedom of choosing the value of p , λ and ϵ . (5) The selection of a certain small p value (in our case $0 < p \leq 0.3$) and precise regulation parameters λ and ϵ improved the approximated scenes even in the noisy environment. Fast calculation to meet the convergence criteria and able to find the global minimum value quickly are other advantage (6) Implementation of this new framework significantly reduced SAR signal sampling, so the load of the onboard system can be reduced as well.

ACKNOWLEDGMENT

The authors would like to thank Mahdi Kartasasmita, senior scientist and former Chairman of Indonesian National Institute of Aeronautics and Space (LAPAN) and reviewers for many valuable comments and suggestions which significantly improved this paper. This research is partially supported by grant No. 1743/UN2.R12/HKP.05.00/2015 from Universitas Indonesia.

REFERENCES

- [1] J. C. Curlander and R. N. McDonough, *Synthetic Aperture Radar: Systems and Signal Processing*. New York, John Wiley & Sons, 1991.
- [2] I. . Woodhouse, *Introduction to Microwave Remote Sensing*. London: CRC Press Taylor & Francis, 2006.
- [3] E. J. Candes and T. Tao, "Near-optimal signal recovery from random projections: Universal encoding strategies?," *IEEE Transactions on Information Theory*, vol. 52, no. 12, pp. 5406–5425, 2006.
- [4] E. J. Candes, J. Romberg, and T. Tao, "Robust uncertainty principles: exact signal reconstruction from highly incomplete frequency information," *IEEE Transactions on Information Theory*, vol. 52, no. 2, pp. 489–509, 2006.
- [5] D. L. Donoho, "Compressed sensing," *IEEE Transactions on Information Theory*, vol. 52, no. 4, pp. 1289–1306, 2006.
- [6] M. A. Herman and T. Strohmer, "High-Resolution Radar via Compressed Sensing," *IEEE Trans. Signal Process.*, vol. 57, no. 6, pp. 2275–2284, Jun. 2009.
- [7] S.-J. Wei, X.-L. Zhang, J. Shi, and G. Xiang, "Sparse reconstruction for SAR imaging based on compressed sensing," *Progress In Electromagnetics Research*, vol. 109, pp. 63–81, 2010.
- [8] R. Arief, D. Sudiana, and K. Ramli, "Compressed Synthetic Aperture Radar Imaging Based On Maxwell Equation," *is accepted and presented in International Conference on 2015 Advanced Research in Electrical and Electronic Engineering Technology (ARIET2015) - 07 - Signal Processing, 24 – 26 November 2015 in Bandung, Indonesia. (All ACCEPTED and REGISTERED papers will be published in the Special Issues in Jurnal Teknologi (Indexed by Elsevier: SCOPUS))*, 2015.
- [9] M. Cheney and B. Borden, *Fundamentals of Radar Imaging*. Society for Industrial and Applied Mathematics, 2009.
- [10] M. Cheney and B. Borden, "Problems in synthetic-aperture radar imaging," *Inverse Problems*, vol. 25, no. 12, p. 123005, 2009.
- [11] B. Sun, Y. Cao, J. Chen, C. Li, and Z. Qiao, "Compressive sensing imaging for general synthetic aperture radar echo model based on Maxwell's equations," *EURASIP Journal on Advances in Signal Processing*, vol. 2014, no. 1, 2014.
- [12] R. Baraniuk and P. Steeghs, "Compressive Radar Imaging," in *Proc. IEEE Radar Conf. 2007*, pp. 128–133.
- [13] J. H. G. Ender, "On compressive sensing applied to radar," *Signal Processing*, vol. 90, no. 5, pp. 1402–1414, 2010.
- [14] V. M. Patel, G. R. Easley, D. M. Healy, and R. Chellappa, "Compressed Synthetic Aperture Radar," *IEEE_J_STSP*, vol. 4, no. 2, pp. 244–254, 2010.
- [15] E. J. Candes, M. B. Wakin, and S. P. Boyd, "Enhancing sparsity by reweighted ℓ_1 minimization," *Journal of Fourier analysis and applications*, vol. 14, no. 5–6, pp. 877–905, 2008.
- [16] R. Chartrand and W. Yin, "Iteratively reweighted algorithms for compressive sensing," in *Acoustics, speech and signal processing, 2008. ICASSP 2008. IEEE international conference on*, 2008, pp. 3869–3872.
- [17] C. E. Shannon, "Communication in the presence of noise," *Proceedings of the IRE*, vol. 37, no. 1, pp. 10–21, 1949.
- [18] Y. C. Eldar and G. Kutyniok, *Compressed Sensing: Theory and Applications*. Cambridge University Press, 2012.
- [19] Z. Ben-Haim, Y. C. Eldar, and M. Elad, "Coherence-based performance guarantees for estimating a sparse vector under random noise," *IEEE Transactions on Signal Processing*, vol. 58, no. 10, pp. 5030–5043, 2010.
- [20] E. Candes and J. Romberg, "L1-magic : Recovery of Sparse Signals via Convex Programming." Caltech, Oct-2005.

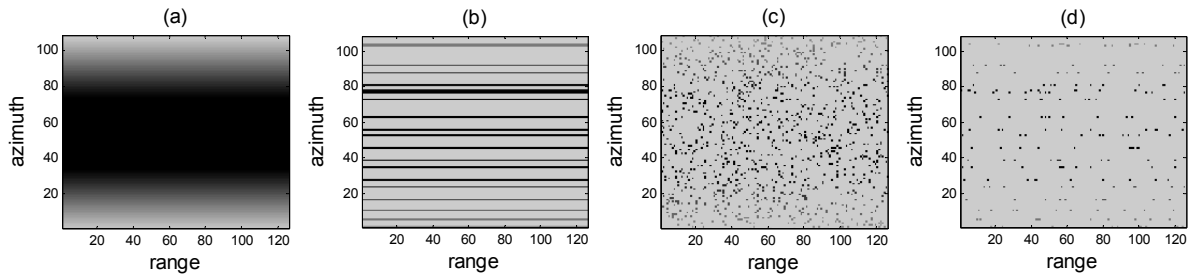


Fig. 1 Compressed SAR signal sampling of target scene (a) full sampling of raw echoes (b) random sampling in slow time (c) random sampling in fast time (d) random sampling in fast time and slow time direction

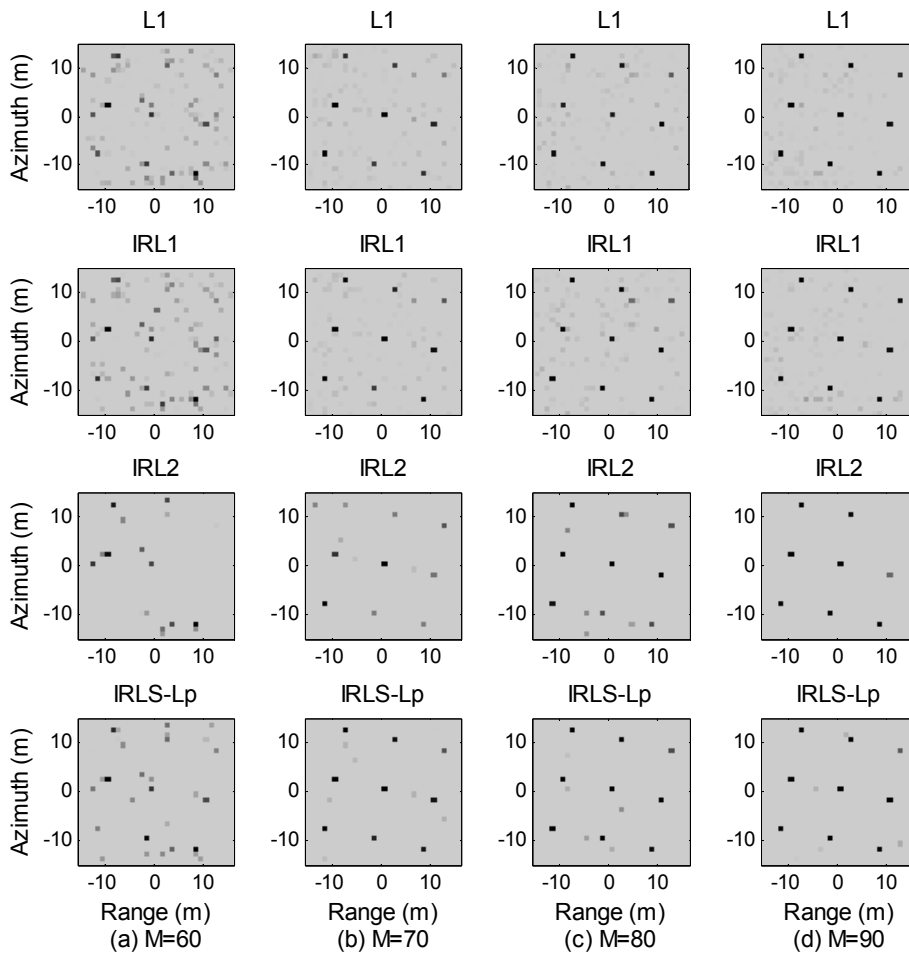


Fig. 2 Result of the approximated scenes using L1, IRL1, IRL2, IRLS-Lp with different numbers of measurements (a) M=60 (b) M=70 (c) M=80 (d) M=90

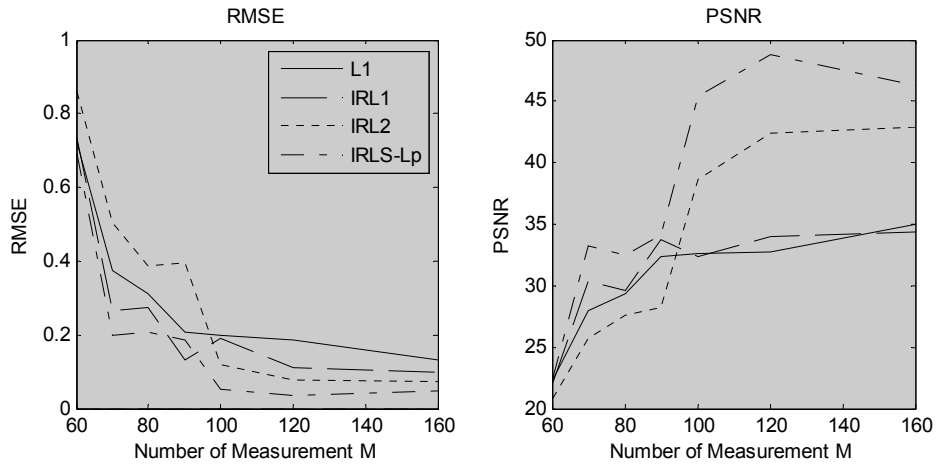


Fig. 3. The RMSE and PSNR value of the approximated scenes using L1, IRL1,IRL2 IRLS-Lp algorithms in different number of measurement M

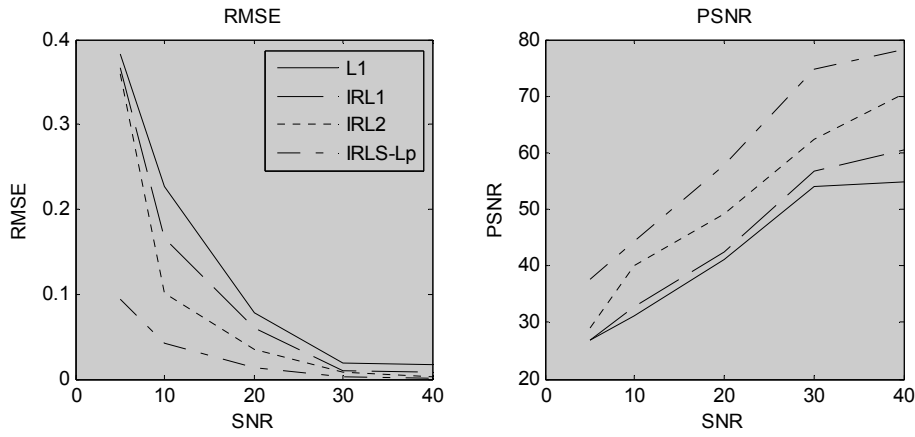


Fig. 4. The RMSE and PSNR value of the approximated scenes using L1, IRL1,IRL2 IRLS-Lp algorithms in different noise level

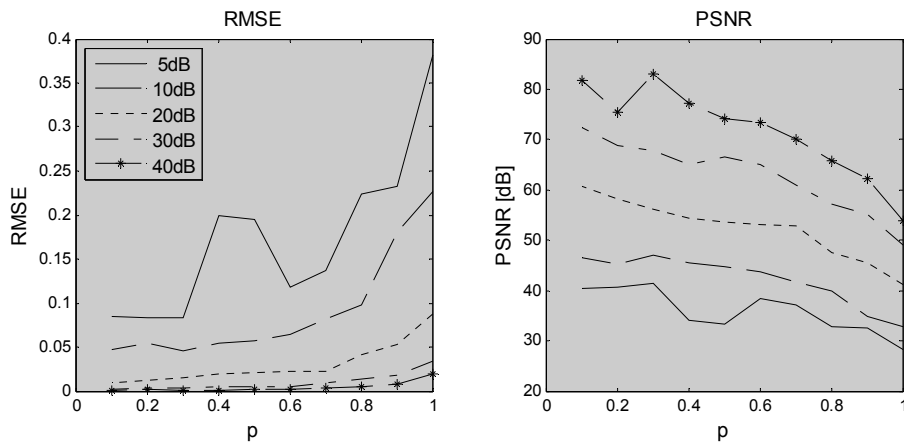


Fig. 5. The effect of p value of the approximated scenes in different noise level

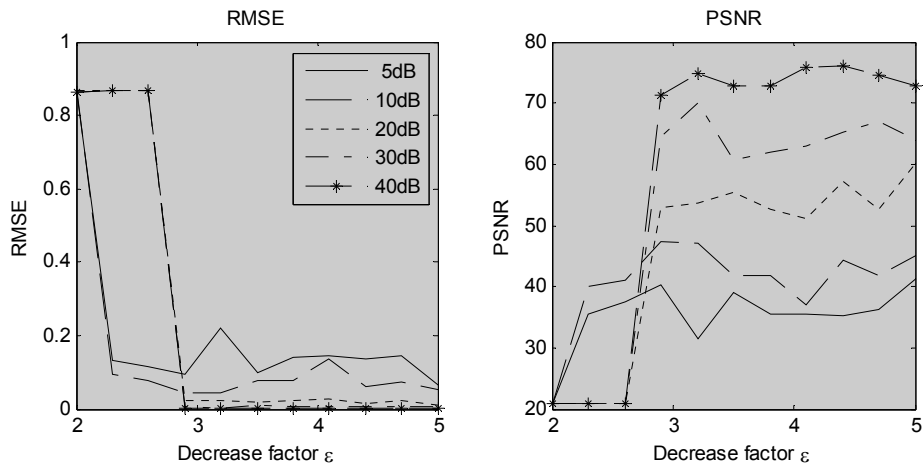


Fig 6 The effect of ϵ to the approximated scenes in different noise level